COMPARISON OF NUMERICAL SCHEMES FOR FOKKER-PLANCK-LANDAU EQUATION. *

CHRISTOPHE BUET[1], STÉPHANE CORDIER[2] AND FRANCIS FILBET[3]

Abstract. This paper is devoted to the comparison of deterministic schemes to approximate the Fokker-Planck-Landau equation. We first recall the basic idea of the spectral and the multigrid methods, and compare them to evaluate their cost, accuracy and robustness. We also present a new method that is very efficient for quasi-isotropic distribution function. We finally implement a method to deal with the numerical simulation in the non homogeneous situation.

AMS Subject Classification. 65M06, 65N06, 82C40 .

.

1. INTRODUCTION

The Fokker-Planck-Landau (FPL) equation is a common kinetic model in plasma physics. It describes binary collisions between charged particles with long-range Coulomb interaction and is represented by a nonlinear partial integro-differential equation. The Fokker-Planck-Landau model is also known as the leading term of classical Boltzmann operator when collisions become grazing.

$$\frac{\partial f}{\partial t} + v.\nabla_x f = Q(f, f), \tag{1}$$

where $Q(f, f)$ is the collision operator:

$$Q(f, f) = \nabla_v . \int_{\mathbb{R}^3} \Phi(v - v^*) \left[(\nabla_v f(t, v)) f(t, v^*) - (\nabla_{v^*} f(t, v^*)) f(t, v) \right] dv^*, \tag{2}$$

with

$$\Phi(v) = |v|^{\gamma+2} S(v), \quad \text{and} \quad S(v) = Id - \frac{v \otimes v}{|v|^2}. \tag{3}$$

The unknown $f(t, x, v)$ represents the density of a gas in phase space of positions x and velocities v, it is non negative and integrable together with its moments up to the second order. As for the Boltzmann equation,

different values of γ lead to usual classification in hard potentials $\gamma > 0$, Maxwellian molecules $\gamma = 0$, or soft potentials $\gamma < 0$. This latter case involves the Coulombian case $\gamma = -3$ which is of primary importance in plasma physics.

As well known in the litterature and mathematically established by the works of Arsene'v, Buryac and more recently Desvillettes [9], the FPL collision operator is the limit of the Boltzmann operator for a sequence of scattering cross sections which converge in a convenient sense to a delta function at zero scattering angle. Concerning the existence of solutions, Arsene'v and Peskov [2] have established the existence of weak solutions for short time in the spacially homogeneous case for the Coulomb potential. Recently, a global existence result of renormalized solution with a defect measure has been obtained by Alexandre and Villani [1, 20] in the space dependance case and for an initial data with a finite energy.

The algebraic structure of the operator is similar to the Boltzmann one, this leads to physical properties such as the conservation of mass, impulsion, and energy

$$\int Q(f,f)(v) \begin{pmatrix} 1 \\ v \\ v^2 \end{pmatrix} dv = 0,$$

and the decay of the kinetic entropy $H(t)$,

$$\frac{dH}{dt}(t) = \frac{d}{dt} \int_{\mathbb{R}^3} f(t,v) \ln(f(t,v)) dv \le 0.$$

Finally, the equilibrium states of the FPL operator, i.e. $Q(f,f) = 0$, are given by maxwellians:

$$M_{\mathcal{N},u_0,T}(v) = \frac{\mathcal{N}}{(2\,\pi\,v_{th}^2)^{3/2}} \exp\left(-\frac{|v-u_0|^2}{2\,v_{th}^2}\right),$$

where $\mathcal{N}$ is the total mass, u_0 the mean velocity, and v_{th} the thermal velocity, which depends on the temperature T, i.e. $v_{th} = \sqrt{\frac{kT}{m}}$, m represents the mass of one particle and k is the Boltzmann constant.

Several numerical approaches have been considered in the last years to deal with the FPL equation in the isotropic case [3] and for cylindrically symmetric problems in [17]. The construction of a conservative and entropy scheme for the general situation has also been proposed by Degond and Lucquin-Desreux in [8]: the starting point of this method is to discretize the collision operator using the weak formulation in order to recover all properties of the continuous operator presented before. But the direct implementation of such a scheme is very expensive, thus several algorithms have been considered to reduce the computational cost as the multipole expansion [12] and the multigrid method [5]. Another approach, based on a direct discretization of the FPL operator using a spectral method has been recently proposed in [14], it permits to reduce the quadratic cost to $N \log N$, where N is the total number of unknowns. In this paper, we shall present a new method based on the approximation of the collision operator for isotropic distribution functions. This approximation is well known in plasma physics [18] for the quasi-isotropic cases and permits us to reduce the cost of the evaluation of the collision operator to a linear complexity.

The spectral and multigrid methods have proved their efficiency in the homogeneous case (the distribution function f does not depend on x), but to the best of our knowledge, there is no numerical result in the non homogeneous situation. Nethertheless, the coupling with the transport part is necessary to treat more physical problem in plasma physics or in rarefied gas dynamic. Moreover, the transport equation creates oscillations or discontinuities in velocity space and the treatment of the collision operator by fast algorithms becomes more complex, then it is necessary to use a robust method to obtain an accurate description of the distribution function. The goal of this paper is to give an algorithm to treat the Vlasov equation coupled with the FPL operator. The transport equation will be solved by a high order semi-lagrangian scheme preserving mass, impulsion, energy and positivity.

The article is organized as follows: in part two, we briefly recall the main features of the fast algorithms, and we derive the so-called isotropic approximation. In the third part, we present some classical numerical tests to compare the accuracy, cost and robustness of different algorithms in the homogeneous case. In the last section, we present a time splitting scheme algorithm to deal with the transport equation. Numerical tests which illustrate the effect of collisions frequency (between free transport and hydrodynamics model) are shown.

2. Three fast algorithms for FPL

This section is first devoted to a brief description of the spectral and multigrid methods. Let us note that the FPL operator is a non linear integro-differential equation, where the non linearity is quadratic in f. However, the complexity of both methods is of order of $N \log(N)$, where N is the number of unknowns.
In the last part, a new method is proposed for the discretization of the FPL equation with a linear cost when the distribution function is almost isotropic.

2.1. The spectral method

This method has been recently proposed by L. Pareschi *et al.* to approximate Boltzmann [15] and Fokker-Planck-Landau [14, 16] equations. We briefly describe the idea of the method and refer to previous references for more details. Let us write the operator on its usual form,

$$Q(f,f) = \nabla_v . \int_{\mathbb{R}^3} \Phi(v - v^*) \left[(\nabla_v f(t,v)) f(t,v^*) - (\nabla_{v^*} f(t,v^*)) f(t,v) \right] dv^*. \tag{4}$$

For simplicity, we will assume the support of the distribution function is included in the ball $B(0, R/2)$ with $R > 0$. Of course, it is wrong since the stationary state is given by a Maxwellian, in fact the distribution function is truncated to zero for f sufficiently small. From this hypothesis, it is easy to check that the domain of integration is $B(0, R)$. We next approximate the distribution by a partial sum of a Fourier series,

$$f_N(t,v) = \sum_{k \in \{-N,..,N\}} \hat{f}_k(t) e^{i \frac{\pi}{R} k.v}, \tag{5}$$

where $k = (k_1, k_2, k_3)$, N is the multi integer (n, n, n), n is the number of half modes in each direction, and the k-th mode is given by

$$\hat{f}_k(t) = \frac{1}{(2\,R)^3} \int_{B(0,R)} f(t,v) e^{-i\,k.v} dv.$$

Then, substituting the approximation $f_N(t,v)$ in the operator (4), we obtain

$$Q(f_N, f_N) = \sum_{l,m \in \{-N,..,N\}^2} \hat{f}_l(t)\, \hat{f}_m(t)\, \hat{\beta}_L(l,m) e^{i \frac{\pi}{R} (l+m).v},$$

where $\hat{\beta}_L(l,m)$ reads to (using a change of variable)

$$\begin{aligned}
\hat{\beta}_L(l,m) &= \left[\frac{\pi}{R}\right]^{\gamma+3} \int_{B(0,\pi)} \Phi(w) \left[(l+m)(l-m) - (l+m).\frac{w}{|w|}(l-m).\frac{w}{|w|} \right] e^{i\,w.m} dw \\
&= \left[\frac{\pi}{R}\right]^{\gamma+3} \left(\hat{B}(l,m) - \hat{B}(m,m) \right),
\end{aligned}$$

and

$$\hat{B}(l,m) = \int_{B(0,\pi)} \|w\|^{\gamma+2} \left[l^2 - (l.\frac{w}{|w|})^2 \right] e^{iw.m} dw.$$

As the residual term of the FPL operator is orthogonal to all trigonometric polynomials of degree $\leq n$, we get the following system of differential equations

$$k \in \{-N, .., N\}, \quad \frac{d\hat{f}_k}{dt} = \left[\frac{\pi}{R}\right]^{\gamma+3} \sum_{\substack{l,m \in \{-N,..,N\} \\ l+m=k}} \hat{f}_l \, \hat{f}_m \left[\hat{B}(l,m) - \hat{B}(m,m)\right].$$

Now, we have to approximate $\hat{B}(l,m)$: we split it in two parts,

$$\begin{aligned}
\hat{B}(l,m) &= \int_{B(0,\pi)} \|w\|^{\gamma+2}\left[l^2 - (l.\frac{w}{|w|})^2\right]e^{iw.m}dw, \\
&= l^2 \int_{B(0,\pi)} \|w\|^{\gamma+2}e^{iw.m}dw - \sum_{i,j=1}^{3} l_i \, l_j \int_{B(0,\pi)} \|w\|^{\gamma+2}\frac{w_i \, w_j}{|w|^2}e^{iw.m}dw.
\end{aligned}$$

and set

$$\begin{aligned}
F(m) &= \int_{B(0,\pi)} \|w\|^{\gamma+2}e^{iw.m}dw \\
I_{i,j}(m) &= \int_{B(0,\pi)} \|w\|^{\gamma+2}\frac{w_i \, w_j}{|w|^2}e^{iw.m}dw,
\end{aligned}$$

to obtain the system of ODE's:

$$\begin{aligned}
\frac{d\hat{f}_k}{dt} &= \left[\frac{\pi}{R}\right]^{\gamma+3} \sum_{m \in \{-N,..,N\}} \hat{f}_{k-m} \, \hat{f}_m \left[(k-m)^2 F(m) - \hat{B}(m,m)\right] \\
&\quad - \left[\frac{\pi}{R}\right]^{\gamma+3} \sum_{i,j=1}^{3} \sum_{m \in \{-N,..,N\}} \hat{f}_{k-m} \, \hat{f}_m (k_i - m_i)(k_j - m_j)I_{i,j}(m).
\end{aligned}$$

Remark 2.1. Coefficients $F(m)$ and $I_{i,j}$ only depend on γ and are approximated using a recursive quadrature formula.

Finally, to approximate the right hand side of the system, we only have to compute several sums of discrete convolutions of the form

$$S_k = \sum_{m \in \{-N,..,N\}} g_m \, h_{k-m}.$$

To do this, we propose a $n^3 \log n^3$ algorithm based on a Fast Fourier Transform:

- use a FFT method to transform g_m and h_{k-m} into $\hat{g}_m$ and $\hat{h}_{k-m}$ with a cost in $O(n^3 \log n^3)$.
- compute the sum in the Fourier space with a linear cost $O(n^3)$.
- use an inverse FFT to obtain the discrete sum with a cost in $O(n^3 \log n^3)$.

The approximation using the spectral method preserves mass, whereas variations of momentum and energy are controled by the spectral accuracy. But, no information is available on the equilibrium states, the decay of the entropy and the preservation of positivity.

2.2. The multigrid method

This method has been proposed by C. Buet *et al.* in [5]. We also assume the domain of integration is a box of length R denoted by C_0, and define for any test function $\varphi(v)$ sufficiently smooth,

$$H(v,v^*) = -\frac{1}{2}f(t,v)f(t,v^*)[\nabla_v\varphi(v) - \nabla_{v^*}\varphi(v^*)]^T \Phi(v - v^*)[\nabla_v \ln(f(t,v)) - \nabla_{v^*} \ln(f(t,v^*))].$$

Then, we write the FPL operator using the weak formulation

$$\int_{\mathbb{R}^3} Q(f,f)(v)\varphi(v)dv = \int_{C_0 \times C_0} H(v,v^*)dv^*dv, \tag{6}$$

and introduce a regular discretization of the box C_0, composed of $N = 8^n$ points, where n will denote the total number of grid levels. The velocity step is denoted by $\Delta v = \frac{R}{2^n}$, and $f_l(t)$ is the approximation of $f(t,v_l)$, where $v_l = l\,\Delta v - v_0$, $l = (l^1, l^2, l^3) \in \mathcal{I} = \{1,..,2^n\}^3$ and v_0 is the center of the box.
We now recall the basic entropy conservative discretization introduced in [8] using the weak form (6), for $l \in \mathcal{I}$, we define $\bar{Q}(f,f)_l$ such that

$$\sum_{l \in \mathcal{I}} \Delta v^3 \bar{Q}(f,f)_l \varphi_l = \sum_{(l,m) \in \mathcal{I}^2} \Delta v^6\, \bar{H}(v_l, v_m),$$

the value $\bar{H}(v_l, v_m)$ is an approximation of $H(v_l, v_m)$ defined for any test sequence φ by:

$$\bar{H}(v_l, v_m) = -\frac{1}{2} f_l(t)\, f_m(t)[(D\varphi)_l - (D\varphi)_m]\Phi(v_l - v_m)[(D\ln f(t))_l - (D\ln f(t))_m], \tag{7}$$

where D is a finite difference operator approximating the gradient.
>From the weak formulation, we finally obtain the following equivalent system of differential equations:

$$\frac{df_l(t)}{dt} = FP_l(t) = (D^*.p(t))_l, \tag{8}$$

where D^* is the formal adjoint of the finite difference operator D, and

$$p_l(t) = \sum_{m \in \mathcal{I}} f_l(t)\, f_m(t)\Phi(v_l - v_m)\Big((D\ln f(t))_l - (D\ln f(t))_m\Big). \tag{9}$$

To obtain the conservation of mass, impulsion and energy, the FPL operator is finally approximated by the average of discrete operators obtained from the down-wind, up-wind and centered finite difference operator D. In [5], authors re-write this scheme as the sum of a second order approximation and an artificial viscosity term in Δv^2 which kills spurious conservations. A direct approximation of (8) is actually too expensive, then to reduce the computational cost, we use a fast algorithm : the multigrid method.
Let us highly recall the algorithm: it consists in splitting the operator in different levels and in computing the interaction betweeen particles on a different way from the relative velocity $|v - v^*|$.
At level one, we only split the domain C_0 in 8 identical boxes denoted by C_1^r, $r \in I_1 = \{0,1\}^3$ and call them the "children of C_0" and C_0 is their "father", then

$$\int_{\mathbb{R}^3} Q(f,f)(v)\varphi(v)dv = \sum_{(r,r') \in \{0,1\}^3} \int_{C_1^r \times C_1^{r'}} H(v,v^*)dvdv^*.$$

At level two, we split each box C_1^r in sub-cells $C_2^{r'}$, for $r' \in I_2 = \{0,1,2\}^3$, then to compute the interactions we introduce the following definition: The cell $C_k^{r'}$ is well separated of C_k^r if and only if their fathers are the nearest neighbors and if $C_k^{r'}$ is not one of the nearest neighbor of C_k^r. The nearest neighbor of C_k^r is obtained by the add to the center the quantities $\frac{R}{2^k}(\varepsilon_1, \varepsilon_2, \varepsilon_3)$, with $(\varepsilon_1, \varepsilon_2, \varepsilon_3) \in \{-1,0,1\}$.
We write the FPL operator as the sum of integral on well separated and not well separated boxes:

$$\int_{\mathbb{R}^3} Q(f,f)(v)\varphi(v) = \sum_{\substack{(r,r') \in I_2 \\ w.s.}} \int_{C_2^r \times C_2^{r'}} H(v,v^*)dvdv^* + \sum_{\substack{(r,r') \in I_2 \\ n.w.s.}} \int_{C_2^r \times C_2^{r'}} H(v,v^*)dvdv^*,$$

where we use the notation $w.s.$ for boxes which are well separated, and $n.w.s$ for the others. If the cell C_2^r is "well separated", we compute the integral using a quadrature formula given below else the contribution is computed at the next level. We repeat this process until the final level n is reached.

For a fixed level k, when C_k^r and $C_k^{r'}$ are well separated, we have to approximate the following integral

$$\int_{C_k^r \times C_k^{r'}} H(v, v^*)dvdv^*, \tag{10}$$

but a direct approximation requires 8^{2k} evaluations which leads to an amount of work in N^2. Therefore, to reduce the computational cost, we only use $n_k = 8^k$ evaluations to approximate (10), and require that after n_k time iterations all the couples $(i, j) \in C_k^r \times C_k^{r'}$ will be chosen: let us denote by $\{1, ..., n_k\}$ the n_k elements of the box C_k^r, and let π be a randomly chosen permutation of $\{1, ..., n_k\}$. In the first step we approximate the integral (10) by a Monte-Carlo quadrature formula using pairs $(l, \pi(l))$, $l \in \{1, ..., n_k\}$, in the second time step we use pairs $(l, \pi^2(l))$, etc... Then after n_k time iterations, the order π is reached.

Finally, when C_k^r and $C_k^{r'}$ are well separated, the Monte-Carlo approximation of (10) is given by

$$\int_{C_k^r \times C_k^{r'}} H(v, v^*)dvdv^* = \frac{1}{2^{n-k}} \sum_{l \in \{1,..,n_k\}} \Delta v^6 H(v_l, v_{\pi(l)}).$$

Then, the computational cost for one evaluation of the FPL operator is reduced to the order $n N$ ($< N \log N$). For the time discretization, a first order Euler scheme is used. To ensure the stability of the algorithm, we determine conditions on the time step Δt under which the scheme gives positive and entropic solution [6]: we first prove there exists a positive constant $C > 0$ such that

$$\left| FP_l(t) \right| = |(D^*p)_l| \leq C \ln(K) f_l(t),$$

where $K = \max_{\{l, |m| \leq 1\}} \frac{f_l}{f_{l+m}}$, then we set $\Delta t_1 = \frac{\alpha}{C \ln(K)}$, with $\alpha \in (0, 1)$, which allows to preserve the positivity of the approximation. Finally, the entropy decays provided that the time step is smaller than

$$\Delta t \leq \min\left(\Delta t_1, \frac{-\Delta v^3 \sum FP_l(t) \ln(f_l(t))}{\Delta v^3 \sum \frac{FP_l^2(t)}{f_l(t)}} \right). \tag{11}$$

Let us notice, that to avoid a global stability condition of the type (11), which may be too restrictive, the operator is split into n parts corresponding to each grid level and the time step is chosen at each level.

2.3. The pseudo-isotropic scheme

The isotropic method for the Fokker-Planck-Landau equation is close to the multigrid method presented before. We are concerned with an approximation of the Fokker-Planck-Landau operator using finite difference. The discretized weak formulation of FPL can be re-written using the symmetry of the operator, for any test function φ

$$\sum_{i \in \mathcal{I}} \frac{\partial f_i}{\partial t} \varphi_i \Delta v^3 = -\Delta v^6 \sum_{(i,j) \in \mathcal{I}^2} f_i f_j (D\varphi)_i \Phi(v_i - v_j)[(D \ln f)_i - (D \ln f)_j], \tag{12}$$

where f_i is any average of f near the cell i (to be defined later), and D denotes the finite difference operator previously used for the multigrid method.

From this finite difference scheme, we finally approximate the following system of ODE's as in (8). When the distribution function is isotropic, one can prove that the multiplicative factor $|v - v^*|^\gamma$ in the matrix Φ can be replaced by $\max(|v|, |v^*|)^\gamma$. This can be checked using an expansion in Legendre polynomials. Indeed, one has

$$\frac{1}{(1 + 2\rho x + \rho^2)^{1/2}} = \sum_{l=0}^{\infty} P_l(x)\rho^l$$

where $\rho = v^+/v^-$ with $v^+ = \max(|v|, |v^*|)$ and $v^- \min(|v|, |v^*|)$ and x is the cosinus of the angle between the two velocities (see [19]). Then, one can see for the continuous equation, that only the zero-th term in this sum gives a non zero contribution. This property is used for deriving the simplified isotropic FPL equation (see [18, 17, 7] for a detailled presentation).

For general distribution function, one can consider a truncated series by retaining only the M first terms in the above expansion. In this paper, one shall consider the coarser approximation ($M = 1$). The positivity and the convergence of this approximation is beyond the scoop of this paper. Using this so called isotropic approximation (which is relevant for distribution function close to isotropic one and exact for isotropic function), we shall improve the scheme described in based on multigrid or multipolar methods [5, 6, 12] : the cost of this method becomes indeed linear and the number of discretization points is no more a power of 2.

Let us now prove that the complexity is linear. We have to evaluate quantities of the form

$$A^{\alpha,\beta,\delta}(v_i) = \sum_j \left(\max(|v_i|, |v_j|)^\gamma f_i f_j (v_i - v_j)_\alpha (v_i - v_j)_\beta ((D \ln f)_i - (D \ln f)_j)_\delta\right), \qquad (13)$$

where α, β and δ are the components in $\{1, 2, 3\}$. These sums are split in two parts provided that either $|v_i| \leq |v_j|$ or not. The first step is to compute the moments but in the "energy" variable $|v|$. Let us define

$$H^{\alpha,\beta,\delta,\varepsilon}(|v_i|) = \sum_j v_{j,\alpha} v_{j,\beta} (D \ln f)_{j,\delta} f_j |v_j|^{\gamma \varepsilon},$$

where the indexes α, β and δ are now in $\{0, 1, 2, 3\}$, ($v_{j,\alpha}$ is the α-th component of v_j if $\alpha \in \{1, 2, 3\}$, else $v_{j,\alpha} = 1$), and the dependance on $|v_i|$ comes from ε which is 0 or 1 (0 for $|v_j| < |v_i|$ and 1 else).

Note that the number of values of the form $|v_i|$ is much smaller than the cardinal of discretization points. For example, if one uses a centrered uniform grid $v_{i,\alpha} = (i_\alpha + 0.5)\Delta v$ where $i_\alpha \in \{-N, N-1\}$, the number of points is $N_1 = 8N^3$ whereas the number of value of $|v_i|$ is less than $3(2N + 1)^2$.

In fact, due to symmetry, there are a multiple of eight velocities for each possible value. In pratice the number of values N_2 which are used is close to $3(2N + 1)^2/10$. Then, the cost of this step is N_1 operations but the cost in storage is N_2. Due to symmetry properties and the structure of the matrix Φ the only quantities that are needed for computing (12) are

$$(\alpha, \beta, \delta) \in \{0, 1, 2, 3\}^3 \text{ such that } \alpha \leq \beta, \ \alpha\beta\delta \notin \{1, 8, 27, 6\}$$

The cardinal of this set is 34.

The second phase is an accumulation phase :

$$F^{\alpha,\beta,\delta}(|v_i|) = f_i \left(|v_i|^\delta H^{\alpha,\beta,\delta,0}(|v_i|) + H^{\alpha,\beta,\delta,1}(|v_i|)\right).$$

This evaluation costs only N_2 operations.

The third part is the attribution part, for example for the term $A^{1,2,2}$ correponding to first row, second column, that is

$$A^{1,2,2}(v_i) = \sum_j \max(|v_i|, |v_j|)^\gamma (v_i - v_j)_1 (v_i - v_j)_2 f_i f_j ((D \ln f)_i - (D \ln f)_j)_2$$

we expand the product of the relative velocity and we obtain

$$
\begin{aligned}
A^{1,2,2}(v_i) \;=\;& \left(v_{i,1}\, v_{i,2}\, F^{0,0,0} \;-\; v_{i,1}\, F^{2,0,0} \;-\; v_{i,2}\, F^{1,0,0} \;+\; F^{2,1,0} \right) (D\ln f)_{i,2} \\
& + \left(v_{i,1}\, v_{i,2}\, F^{0,0,2} \;-\; v_{i,1}\, F^{2,0,2} \;-\; v_{i,2}\, F^{1,0,2} \;+\; F^{2,1,2} \right)
\end{aligned}
$$

The cost of this last part is N_1, and we can compute the approximation $p_{i,1}(t)$ defined by (9):

$$
p_{i,1}(t) = A^{2,2,1}(v_i) + A^{3,3,1}(v_i) - A^{1,2,2}(v_i) - A^{1,3,3}(v_i)
$$

In conclusion, we prove that the evaluation of double integral of the form (13) has a linear complexity despite of its quadratic structure. The second advantage when using this approximation is that the number of points is no more of the form 2^k. This is also very important for the flexibility of the method.

3. Numerical tests in the homogeneous case:

We now present numerical tests to compare the algorithms in different cases:

- the Maxwellian case ($\gamma = 0$) for which explicit solutions are known [4, 13].

- the Coulombian isotropic case ($\gamma = -3$) introduced in [18] for which a one dimensional isotropic code [7] is used to compute reference solutions.

- the Coulombian bi-maxwellian case: this last test is of primary importance in plasma physics and consists of an initial bi-maxwellian distribution which is far to be isotropic. Therefore, only the two first methods have been compared. We consider discretizations for which the total CPU time is the same.

In these tests, we will consider the time evolution of the following quantities:

- Discrete kinetic entropy:
$$
H(t) = \sum_{i\in\mathbb{Z}^3} \Delta v^3\, f_i(t)\, \ln(f_i(t)).
$$

- Discrete moment of order 4:
$$
M_4(t) = \sum_{i\in\mathbb{Z}^3} \Delta v^3\, |v_i|^4\, f_i(t).
$$

- Discrete temperatures:

$$
\text{for k=1,2,3,} \quad T_k(t) = \sum_{i\in\mathbb{Z}^3} \Delta v^3\, (i^k\,\Delta v - u_0^k)^2 f_i(t), \quad \text{and} \quad T(t) = \frac{1}{3}\sum_{k=1}^{3} T_k(t),
$$

where $u_0 = (u_0^1, u_0^2, u_0^3)$ is an approximation of the impulsion $\frac{1}{\mathcal{N}} \int_{\mathbb{R}^3} v\, f(t,v)dv$, and $\mathcal{N}$ an approximation of the total mass.

- Quadratic error: for the Maxwellian case we are able to compute an explicit solution, we denote by f^{exact} the solution of the Fokker-Planck-Landau equation, and define the discrete L^2 norm error by,

$$
EQ(t) = \frac{\left(\sum \Delta v^3\, |f^{exact}(v_i,t) - f_i(t)|^2 \right)^{1/2}}{\left(\sum \Delta v^3 |f^{exact}(v_i,t)|^2 \right)^{1/2}}.
$$

We will consider three test cases, namely

Number of unknowns	spectral method	multigrid method	pseudo-isotropic method
$16 \times 16 \times 16$	0.4 sec	0.08 sec	0.03 sec
$32 \times 32 \times 32$	10 sec	1.8 sec	0.37 sec

TABLE 1. *Computation time for spectral, multigrid and pseudo-isotropic methods with respect to the number of unknowns for one evaluation of the FPL operator (TEST 1).*

Number of unknowns	spectral method	multigrid method	pseudo-isotropic method
$16 \times 16 \times 16$	2 min 40 sec	10 sec	03 sec
$32 \times 32 \times 32$	07 h 40 min	3 min 21 sec	1 min 50 sec

TABLE 2. *Total computation time for spectral, multigrid and pseudo-isotropic methods with respect to the number of unknowns (TEST 1).*

3.1. The Maxwellian case ($\gamma = 0$)

The initial data is chosen on the class of known exact isotropic solutions which is an extension of Bobylev solutions [4]: we set $S = 0.6$ and consider

$$f_0(v) = \frac{1}{(2\,\pi\,S)^{3/2}} \frac{1-S}{S} \frac{|v|^2}{2\,S} \exp(-\frac{|v|^2}{2\,S}).$$

Numerical results are compared with the explicit solution

$$f(t,v) = \frac{1}{(2\,\pi\,S)^{3/2}} \left(\frac{5\,S-3}{2\,S} + \frac{1-S}{S} \frac{|v|^2}{2\,S} \right) \exp(-\frac{|v|^2}{2\,S}),$$

where $S = 1 - 0.4 \exp(-t/6)$.

In this case the temperatures $T_1(t)$, $T_2(t)$, $T_3(t)$ are equal because of the isotropy of the solution. This test is carried out to check the accuracy by comparing the quadratic error using the multigrid and the pseudo-isotropic methods with 16^3 and 32^3 points and a time step $\Delta t = 0.1$ whereas the spectral method is used with 16^3 modes with $\Delta t = 0.1$ and 32^3 modes with $\Delta t = 0.016$. A fourth order Runge-Kutta scheme for the time discretization is used to keep the high accuracy of the method. It is also important to mention that the support of the initial distribution function for the spectral method is much larger than one used for the multigrid scheme, indeed to obtain stability and to avoid aliasing effect inherent to the method a sufficiently large support has to be used. The simulation is stopped when stationary state is achieved i.e. variations of entropy are negligible. The Table 1 shows the computation time for the evaluation of the collision operator, the cost is highly reduced with the pseudo-isotropic code. In Table 2, we give the total time of computation for different methods with respect to the number of unknowns. The increase of the computation time for the spectral method with 32^3 modes is due to the use of a fourth order time solver which needs four evaluations at each time step. Moreover, the stability condition is of order $O(\frac{1}{N^2})$, where N is the number of unknowns, and is very restrictive for this resolution. A fourth order Adams-Balshforth scheme, which only needs one evaluation by iteration, has also been tested but the restriction on the time step is too important to have a gain. On the other hand the sub-cycling algorithm used for the multigrid method is very efficient for this test. The linear cost of the pseudo-isotropic scheme allows to improve the CPU time even if the stability condition remains quadratic, i.e. $\Delta t \leq C\,\Delta v^2$.

The evolution of the discrete error norm, the entropy and the fourth order moment are plotted (see Figures 1,2,3). In view of these results, the multigrid method and the pseudo-isotropic scheme seem to be first order accurate, indeed even if the finite difference approximation of the gradient is second order, the use of the Monte-Carlo algorithm for the multigrid method reduces the accuracy. On the opposite, the spectral method is much more accurate with 32^3 modes and seems to be at least second order. Let us note that the evolution of the discrete error norm induced by the spectral method using 16 modes is only four times larger than the one induced by the multigrid method with 32 points in each direction. But the error obtained by the spectral method does not converge to zero when t goes to infinity, which means that the stationary state is not well described. Moreover, the behavior of the entropy and the fourth order moment for the spectral method using 16^3 modes is not sufficiently accurate, while the evolution obtained by the multigrid method is smooth with only 16 points per direction.
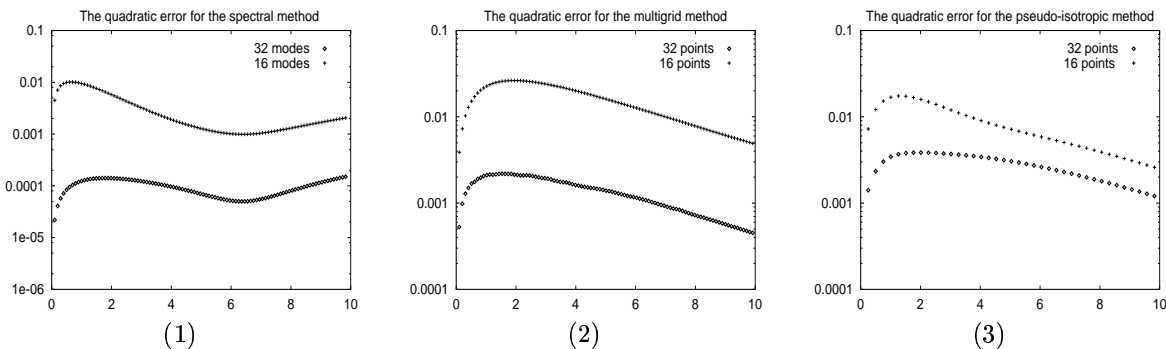

FIGURE 1. *Evolution of the relative quadratic error for (1) the spectral method, (2) the multigrid method, (3) the pseudo-isotropic scheme using 16^3 and 32^3 unknowns (TEST 1).*
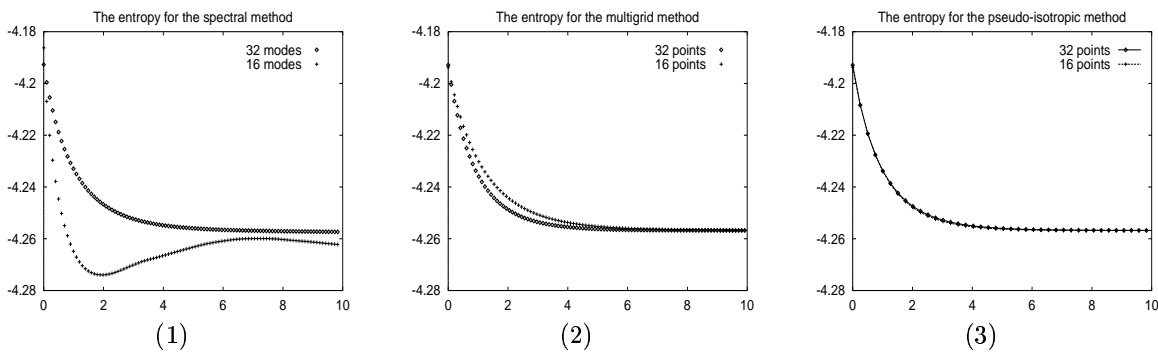

FIGURE 2. *Evolution of the entropy for (1) the spectral method, (2) the multigrid method, (3) the pseudo-isotropic scheme using 16^3 and 32^3 unknowns (TEST 1).*

3.2. The Isotropic case ($\gamma = -3$)

The initial data is now chosen to be isotropic:

$$f_0(v) = \frac{1}{S^2} \exp\left(-S \frac{(|v| - \sigma)^2}{\sigma^2}\right)$$
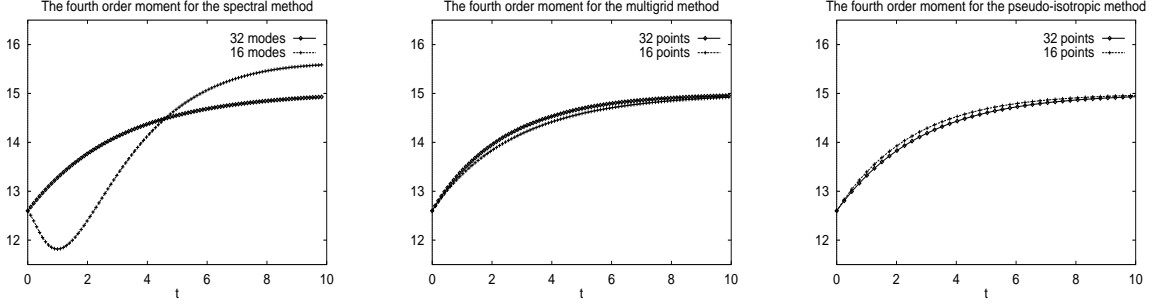
FIGURE 3. *Evolution of the fourth order moment for (1) the spectral method, (2) the multigrid method, (3) the pseudo-isotropic scheme using 16^3 and 32^3 unknowns (TEST 1).*

with $S = 10$, $\sigma = 0.3$. This test is performed to compute the evolution of entropy and to compare it with results obtained by the isotropic code, described in [7], which is used with a large number of points representing the energy variable $\varepsilon^2 = |v|^2$. The spectral method is only used with 16^3 modes whereas we take 32^3 points for the multigrid and pseudo-isotropic methods.

In view of Figures 4 and 5, the evolution of the entropy induced by both methods is in good agreement with one obtained by the isotropic code. Note that to avoid aliasing effect a large support of the initial data is needed for the spectral method, then the description of the distribution function is less accurate than one obtained by the multigrid method, but the stationary state is well described by both methods. The pseudo-isotropic code also gives nice results in this case since the solution remains isotropic.
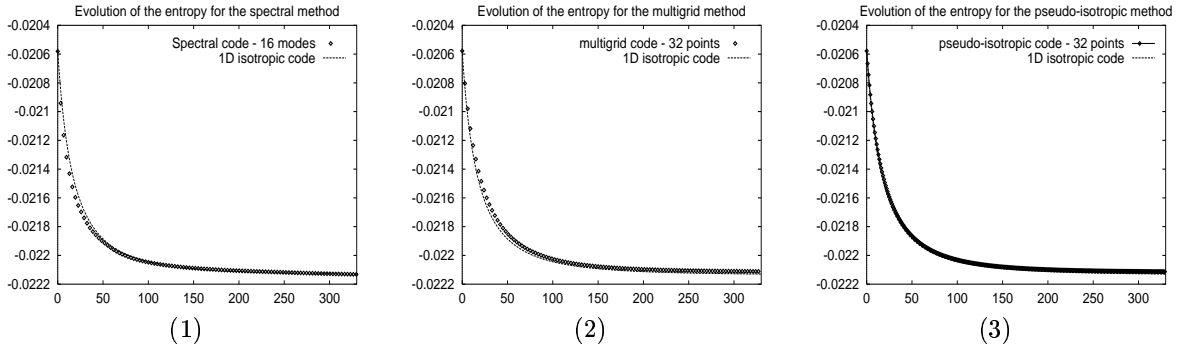

FIGURE 4. *Entropy evolution for (1) the spectral method, (2) the multigrid method, (3) the pseudo-isotropic scheme, compared with the one obtained by the 1d isotropic code (TEST 2).*

3.3. The sum of two gaussians ($\gamma = -3$)

The initial data is now chosen to be bimaxwellian, i.e. a sum of two Maxwellian functions:

$$f_0(v) = \frac{1}{2}\Big(\mathcal{M}_{\mathcal{N},v_1,T}(v) + \mathcal{M}_{\mathcal{N},v_2,T}(v)\Big)$$

with $v_1 = (2,3,3)$, $v_2 = (4,3,3)$, and $v_0 = (3,3,3)$ is the center of the domain. The final time of the simulation is $T = 20$ for which the equilibrium state is reached. The thermal velocity is equal to $v_{th} = 0.45$, and the total mass is $\mathcal{N} = 5$. This test is used to compute the relaxation of the entropy, the temperature and the distribution function.
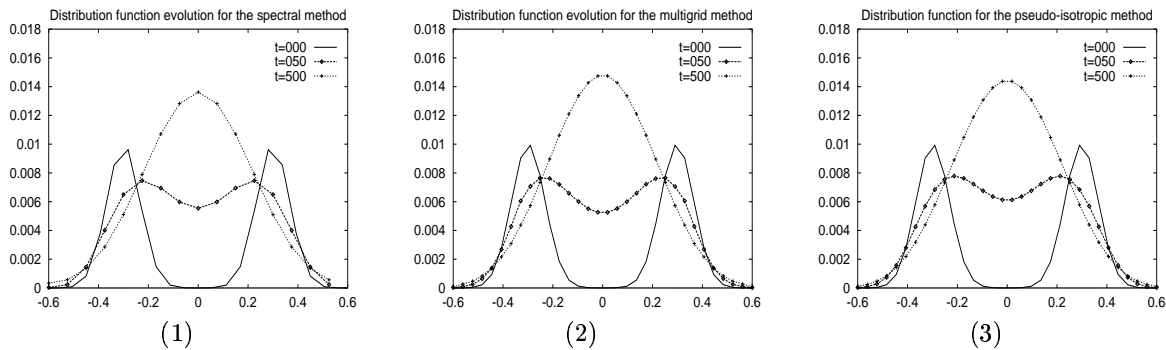
FIGURE 5. *Evolution of the distribution function for (1) the spectral method, (2) the multigrid method, (3) the pseudo-isotropic scheme (TEST 2).*

Number of unknowns	spectral method	multigrid method
$8 \times 8 \times 8$	0.03 sec	
$16 \times 16 \times 16$	0.40 sec	0.08 sec
$32 \times 32 \times 32$	9.00 sec	1.88 sec

TABLE 3. *Computation time for the spectral and the multigrid method with respect to the number of unknowns for one evaluation of the FPL operator (TEST 3).*

We first present (see Table 3) the computation time for one iteration with an Euler scheme in order to compare the time required for one evaluation of the collision operator by spectral and multigrid methods. The increase of the computational cost of methods is in good agreement with the theoretical prediction in $N \log N$, where N is the number of unkowns. But, the computation time required for the evaluation of the operator with the multigrid method is highly reduced compared to the spectral one.

The CPU time for the complete simulation is listed on Table 4, for this test we use 8^3 and 16^3 modes for the spectral method, and 16^3, 32^3 grid points for the multigrid scheme. The computation time is very close when the multigrid algorithm is used with 32^3 points and the spectral one with only 16^3 modes. In the following figures, we present the evolution of physical quantities obtained by both methods. To keep the high order accuracy of the spectral method, a fourth order Runge-Kutta scheme is required, thus a few number of modes is sufficient to obtain satisfying results: the relaxation of the temperature (Figure 6) obtained by the multigrid method using 32^3 points is in good agreement with one obtained by the spectral algorithm using only 16^3 modes, even if the equilibrium state of the temperature is more accurate with the multigrid method. Moreover, in view of results given in Figure 7, the entropy obtained by the spectral algorithm (which is not an entropic scheme) is decreasing and as accurate as one obtained by the multigrid method. The evolution of the fourth order moment generated by the spectral method is still increasing, but the stationary state is well described by both methods (see Figure 8).

4. THE NON HOMOGENEOUS CASE

The goal of this section is to give an efficient algorithm to solve the non homogeneous equation:

$$\frac{\partial f}{\partial t} + v \cdot \nabla_x f = Q(f, f) \tag{14}$$

spectral method	CPU time	multigrid method	CPU time
$8 \times 8 \times 8$	3 min 57 sec	$16 \times 16 \times 16$	1 min 52 sec
$16 \times 16 \times 16$	33 min 04 sec	$32 \times 32 \times 32$	36 min 53 sec

TABLE 4. *Total computation time for the spectral (resp. multigrid) method with respect to the number of modes (resp. points) (TEST 3).*
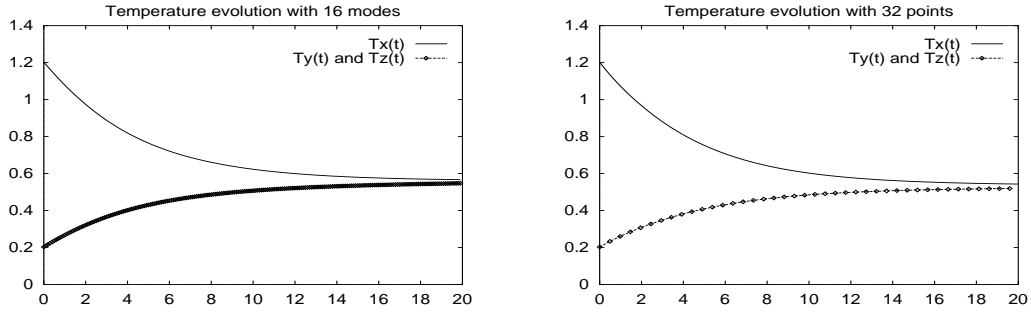

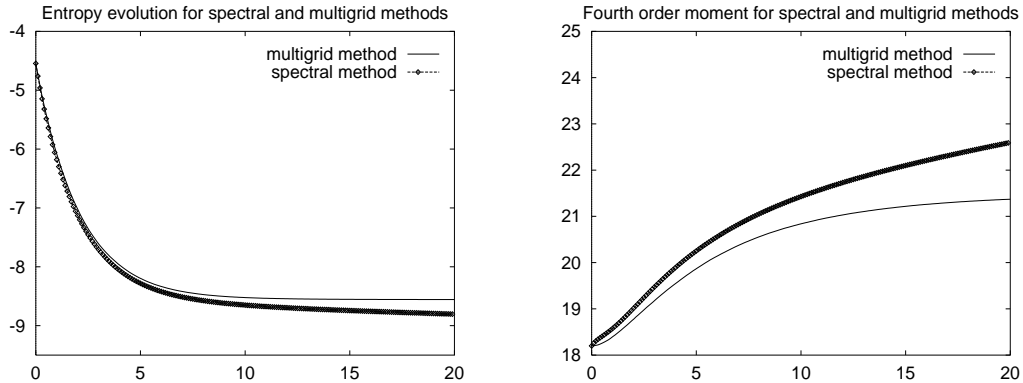FIGURE 6. *Temperature evolution for the spectral (left) and the multigrid (right) methods (TEST 3).*

FIGURE 7. *Entropy (left) and fourth order moment (right) evolution for the spectral method using 16^3 modes and for the multigrid method with 32^3 points (TEST 3).*

We use the classical time splitting scheme: assume $f^n(x, v)$ is an approximation of f at time t^n, we first discretize the free transport problem,

$$
\begin{cases}
\dfrac{\partial f}{\partial t} + v \,.\nabla_x f = 0, & \text{for } t \in [0, \Delta t], \\[2mm]
f(0, x, v) = f_h^n(x, v),
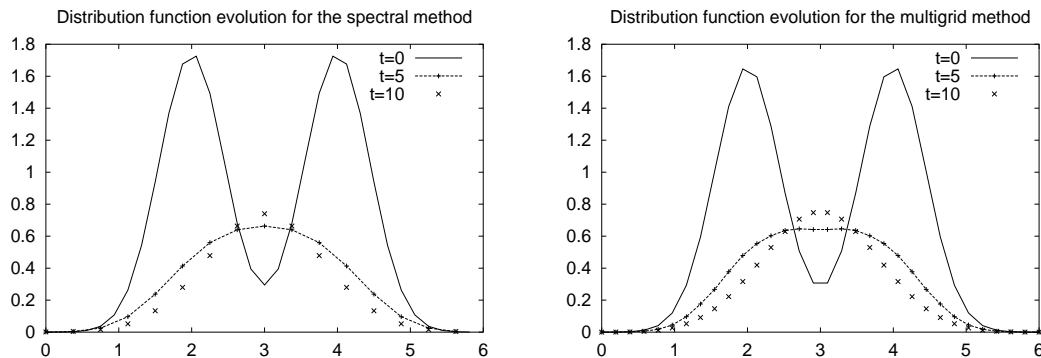\end{cases}
\tag{15}
$$

FIGURE 8. *Evolution of the distribution function for the spectral (left) and the multigrid (right) methods (TEST 3).*

and, the collision part using a fast algorithm,

$$\begin{cases} \dfrac{\partial \tilde{f}}{\partial t} = \dfrac{1}{k}\, Q(\tilde{f}, \tilde{f}), & \text{for } t \in [0, \Delta t], \\[3mm] \tilde{f}(0, x, v) = f(\Delta t, x, v). \end{cases} \tag{16}$$

where k is the Knudsen number linked to the collision frequency. From the numerical tests presented in the previous section, the multigrid method seems to be more suitable for computations in the non homogeneous case. Indeed, the computational cost is highly reduced compared to the spectral method for the three dimensional problem, even if it is only first order accurate. Moreover, the sub-cycling algorithm for the time discretization allows to use large time step, then it is possible to treat problems with small Knudsen numbers.

4.1. **Discretization of the transport equation**

In this section, we present a numerical scheme based on a Lagrange-Galerkin method to deal with the transport equation (15). For simplicity, we will restrict ourselves to a one dimensional problem, but the algorithm can be easily extended to higher dimensions. Let (x_{min}, x_{max}) be the computational domain, we denote by n_x the number of cells of the mesh, the space step $\Delta x = (x_{max} - x_{min})/n_x$, x_i is the center of the cell $C_i = (x_{i-1/2}, x_{i+1/2})$, with $x_{i+1/2} = x_i + \frac{\Delta x}{2}$.
We now assume $f_h^n(., v)$ is a piecewise constant function approximating the average of the distribution function $f(t^n, ., v)$ on each cell C_i, $i \in \{0, .., n_x - 1\}$,

$$f_h^n(x, v) = f_i^n(v) \sim \frac{1}{\Delta x} \int_{x_{i-1/2}}^{x_{i+1/2}} f(t^n, x, v)dx$$

The numerical scheme proposed can be split in three steps: the reconstruction, the resolution and the cell-averaging step.
Let us assume that v is fixed and positive (here, the variable v acts as a parameter, and will be omitted in the reconstruction part). The use of the method of reconstruction via primitive function allows to obtain a high order approximation of the distribution function. For example, we set F^n be a primitive of the distribution

function f_h^n, then we have for all i, $F^n(x_{i+1/2}) - F^n(x_{i-1/2}) = \Delta x f_i^n$, and

$$F^n(x_{i+1/2}) = \Delta x \sum_{k=0}^{i} f_k^n = w_i^n.$$

On the cell C_i, we first compute the polynom of degree three interpolating the primitive F^n at points $\{x_{i-1/2}, x_{i+1/2}, x_{i+3/2}\}$. By differentiation, we obtain a first approximation

$$\tilde{f}_h(x) = \frac{d F^n}{dx} = f_i^n + \frac{(x - x_i)}{\Delta x} \Delta f_i^n, \quad \text{with } \Delta f_i^n = f_{i+1}^n - f_i^n.$$

Finally, we introduce slope correctors to ensure the positivity of the numerical reconstruction:

$$f_h(x) = f_i^n + \frac{(x - x_i)}{\Delta x} \epsilon_i \, \Delta f_i^n,$$

where

$$\epsilon_i = \begin{cases} \min\left(1, 2\frac{f_i^n}{\Delta f_i^n}\right) & \text{if } \Delta f_i^n > 0 \\ \\ \min\left(1, -2\frac{f_\infty - f_i^n}{\Delta f_i^n}\right) & \text{if } \Delta f_i^n < 0 \end{cases}$$

where $f_\infty = \max_{i=\{0,..,n_x\}}\{f_i^n\}$. The parameter ϵ_i allows to preserve the positivity and to eliminate spurious oscillations. A classical slope limiter (minmod, superbee) also allows to preserve positivity but introduces dissipation giving a strong decay of the entropy, which is theoretically conserved by the transport step.

Now, the resolution step consists in approximating the characteristic curves corresponding to the transport equation. In this case, the solution can be explicitly computed since the characteristic curves become straight lines

$$f_h(t^{n+1}, x) = f_h(t^n, x - v\Delta t).$$

This method allows to avoid a CFL condition which can be very restrictive since the velocity support is large. Finally, the average on the cell C_i at time t^{n+1} is computed

$$f_i^{n+1} = \frac{1}{\Delta x} \int_{x_{i-1/2}}^{x_{i+1/2}} f_h(t^n, x - v\Delta t)dx.$$

This leads to the following scheme

$$f_i^{n+1} = f_{i-j}^n - \frac{1}{\Delta x}(\phi_{i-j+1/2}^n - \phi_{i-j-1/2}^n).$$

with

$$\phi_{i-j+1/2}^n = \int_{x_{i-j+1/2}-\alpha}^{x_{i-j+1/2}} f_h(x)dx,$$

$j = \left[\frac{v\Delta t}{\Delta x}\right]$, where [.] represents the integer part and $\alpha = v\,\Delta t - j\,\Delta x$, then we obtain

$$\phi_{i-j+1/2}^n = \alpha \left[f_{i-j}^n + \frac{1}{2}(1 - \frac{\alpha}{\Delta x}) \epsilon \Delta f_{i-j}^n\right].$$

This numerical scheme preserves the positivity, indeed the use of slope correctors ensure the positivity of the reconstructed approximation, and the resolution and cell-averaging steps are obviously positive. Moreover, the approximation satisfies:

$$\sum_i f_i^{n+1}(v) \begin{pmatrix} 1 \\ v \\ v^2 \end{pmatrix} = \sum_i f_i^n(v) \begin{pmatrix} 1 \\ v \\ v^2 \end{pmatrix}.$$

4.2. **Numerical tests:**

4.2.1. *The bi-maxwellian test case:*

We first consider an initial data which is bi-maxwellian with a strong modulation of the density

$$f_0(x,v) = \frac{1}{2}\Big(\mathcal{M}_{\mathcal{N},v_1,T}(v) + \mathcal{M}_{\mathcal{N},v_2,T}(v)\Big)\Big(1 + 0.5\,\cos(k_0\,x)\Big).$$

with $k_0 = 0.3$. For simplicity we consider periodic boundary conditions in x

$$f(t,0,v) = f(t,L,v), \quad \forall (t,v) \in \mathbb{R}^+ \times \mathbb{R}^3.$$

Under this condition, mass, impulsion and energy are conserved and the stationary state is given by the Maxwellian obtained from the total mass, velocity and total temperature of the initial data. This test is achieved to check the evolution of temperature and entropy in the non homogeneous case (see Figure 9). Total temperature is well conserved, and entropy is first exponentially decreasing and is finally stabilized to the value of the entropy of the Maxwellian at the stationary state. In Figure 10, the evolution of the distribution function in the phase space (x, v_x) obtained by integrating in (v_y, v_z) is plotted: the transport equation with periodic boundary conditions induces oscillations in the velocity space, but after some iterations, the collision operator acts as a diffusion equation which kills oscillations and leads to the the stationary state.
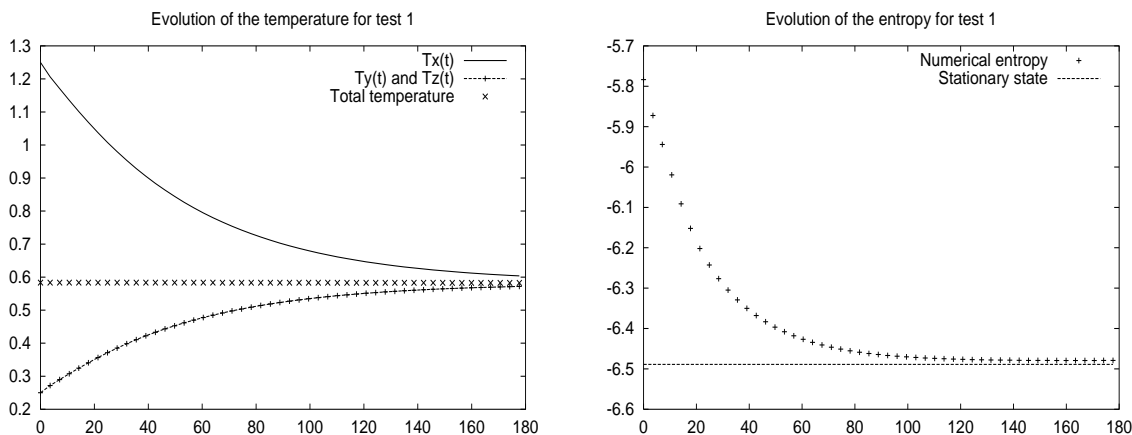

FIGURE 9. *Évolution of the temperature (left) and the entropy (right) for the non homogeneous case (TEST 1).*

4.2.2. *The shock tube: from free transport to hydrodynamics models.*

In this example, we are interested in gas dynamic problems, then the evolution of macroscopic quantities is observed: $\rho(t, x)$ represents the gas density, $u(t, x)$ is the gas velocity, and $T(t, x)$ is the total temperature of the gas. These macroscopic quantities are obtained by computing moments of the distribution function $f(t, x, v)$
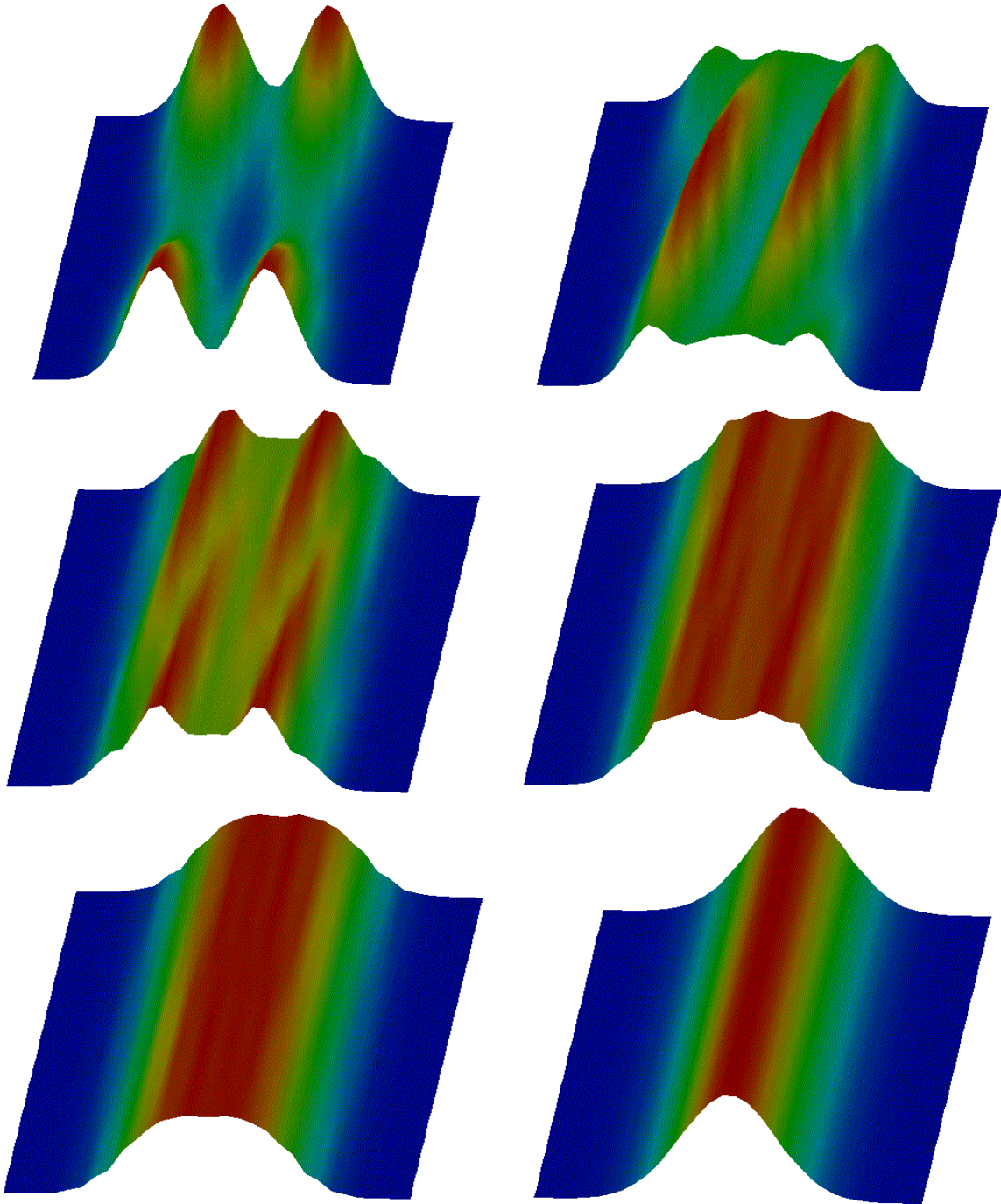
FIGURE 10. *Evolution in time of the distribution function for the non homogeneous case in the* (x, v_x) *space (TEST 1).*

with respect to the variable v.

Then, we discretize the non homogeneous equation:

$$\frac{\partial f}{\partial t} + v_x \frac{\partial f}{\partial x} = \frac{1}{k} Q(f, f),$$

where k is the Knudsen number, which determines the frequency of collisions. We present simulations for different Knudsen numbers and compare macroscopic values (ρ, u, T) obtained by the numerical scheme with the approximated solution of the free transport (without collision) and with the numerical solution of Euler equations which are hydrodynamic limit of the Boltzmann equation in gas dynamics:

$$\begin{cases} \dfrac{\partial \rho}{\partial t} + \dfrac{\partial}{\partial x}(u\,\rho) = 0, \\[2mm] \dfrac{\partial}{\partial t}(\rho\,u) + \dfrac{\partial}{\partial x}(\rho\,u^2 + p) = 0, \\[2mm] \dfrac{\partial}{\partial t}(\rho\,e) + \dfrac{\partial}{\partial x}(\rho\,e + p)\,u = 0. \end{cases}$$

with an equation of state to close the system, here we will consider an ideal gas.

Let us consider the initial conditions from Sod's shock tube problem

$$\begin{cases} (\rho_l, u_l, T_l) = (1, 0, 1) & \text{if } 0 \le x \le 0.5, \\[2mm] (\rho_r, u_r, T_r) = (0.125, 0, 0.25) & \text{if } 0.5 < x \le 1, \end{cases}$$

>From this quantities, we compute the initial data given by a

$$\begin{cases} f_0(x, v) = M_{\rho_l, u_l, T_l} & \text{if } 0 \le x \le 0.5, \\[2mm] f_0(x, v) = M_{\rho_r, u_r, T_r} & \text{if } 0.5 < x \le 1, \end{cases}$$

The solution starts with a hot high density gas in the region $0 \le x \le 0.5$, and a cold low density gas in the region $0.5 \le x \le 1$. The gas is initially at rest. At $t = 0$ the diaphragm separating two regions is removed, causing a shock wave to propagate into the low density medium and a rarefaction wave into the high density medium.

We observe that when the Knudsen k number goes to zero, the macroscopic values (ρ, u, T) are close to the solution of Euler equations. Moreover, the distribution function solution of the free transport equation ($k = +\infty$) develops large gradients in velocity, whereas a smoother profile in v is obtained when the Knudsen number k goes to zero (see Figure 11).

5. CONCLUSION

In this paper, we have reviewed and compared the spectral and multigrid methods and have presented a new method to approximate the FPL operator in the pseudo-isotropic case. This last method drastically reduces the computational cost, but cannot be applied when the distribution function is too far from the isotropy.

The spectral method only conserves mass, but gives an approximation of momentum and energy with the spectral accuracy provided that the support is large enough. A compromise has to be found on the size of the support to obtain a good accuracy and to avoid aliasing effect. Numerical tests show that the variations of moments are negligible, but the computational cost is still too important to use a sufficiently large number of
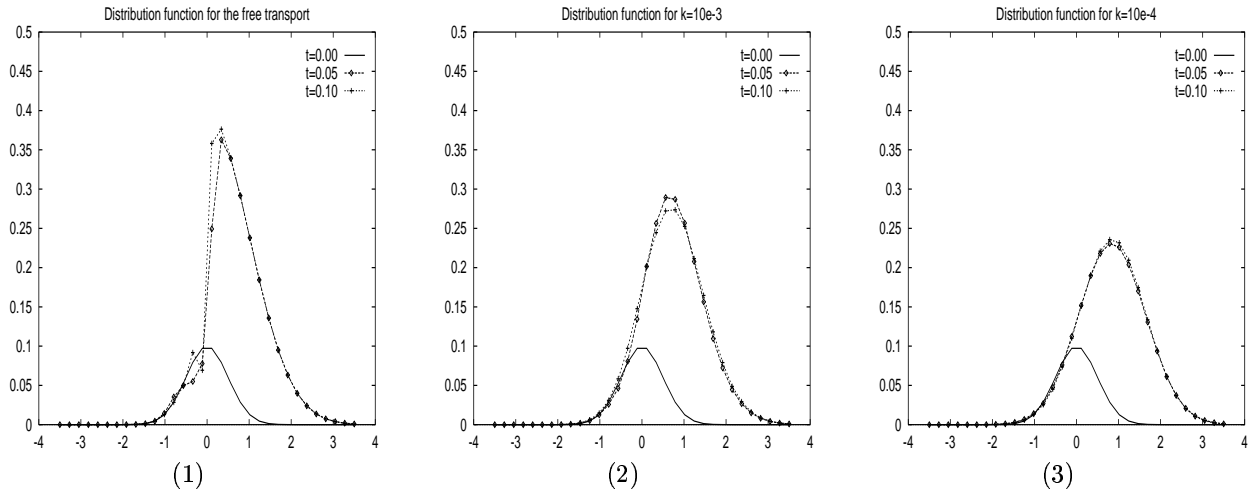
FIGURE 11. *Evolution of the distribution function at* $x = 1/2$ *for (1) the free transport, for (2) the FPL equation with* $k=10^{-3}$ *and (3)* $k=10^{-4}$ *(right) (TEST 2).*
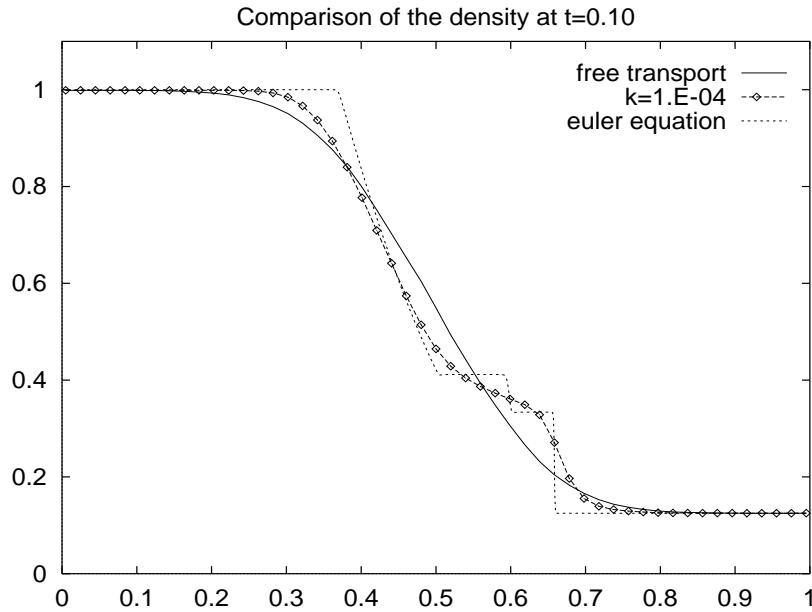

FIGURE 12. *Density for the free transport equation, the FPL operator with* $k=10^{-4}$ *and the Euler system at time* $t = 0.10$ *(TEST 2).*

modes or to treat the non-homogeneous equation in three dimensional velocity space. Moreover, the stability condition on the time step is of order $O(\frac{1}{N^2})$, where N is the number of unknowns in v. Let us note that a third order DUMKA scheme [11] has been used for the two dimensional computation of the FPL operator and allows us to reduce the cost of the method. Then, in this case the non homogeneous equation can be also treated [10]. Finally, the high order accuracy of the spectral method is particulary useful for short time simulation.

Concerning the multigrid method coupled with the finite difference scheme preserving moments, it gives satisfying results with a few number of points and with a reasonable cost. Indeed, the sub-cycling algorithm,
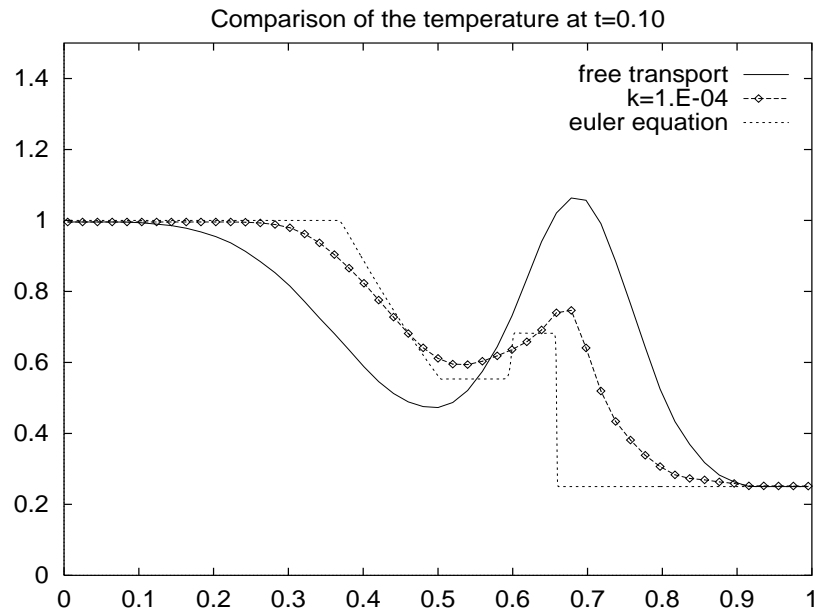
Comparison of the temperature at t=0.10

FIGURE 13. *Temperature for the free transport equation, the FPL operator with k=10^{-4} and the Euler system at time t = 0.10 (TEST 2).*
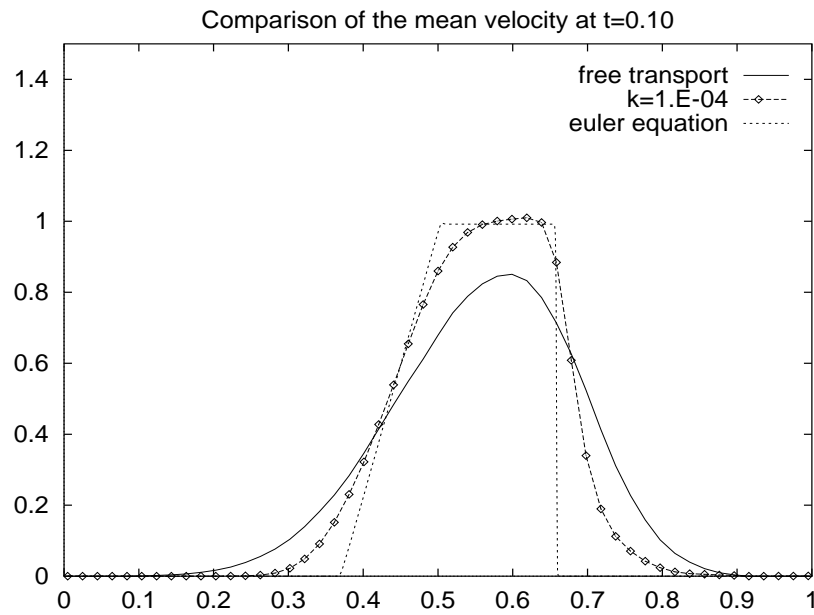
Comparison of the mean velocity at t=0.10

FIGURE 14. *Mean velocity for the free transport equation, the FPL operator with k=10^{-4} and the Euler system at time t = 0.10 (TEST 2).*

avoiding a global stability condition on the time step, allows to highly reduce the computational cost. Moreover, the conservation of moments and the preservation of positivity seem to be necessary for long time simulation. The monte-Carlo formula considerably reduces the accuracy of the method, but it is sufficient to treat the full problem in the non homogeneous case. Finally, let us remark that for the shock tube test, the solution remains isotropic near the boundary, then in this case the pseudo-isotropic scheme could be used to reduce the cost of the method.

The discretization in time with pseudo-isotropic method needs to be optimized : note that the subcycling strategy used for multigrid method (see [5, 6]) is not easy to adapt. Let us point out that this method is optimal for the CPU time point of view : its cost is linear and the number of points is not restricted to some power of 2.

References

[1] R. Alexandre, C. Villani. On the Landau approximation in plasma physic. *preprint ENS Ulm.*, (2000).

[2] A. A. Arsenev, N. V. Peskov. On the existence of a generalized solution of Landau equation. *U.S.S.R. Comput. Maths. Math. Phys.*, 17, No.4, (1977) pp. 241–246.

[3] A. V. Bobylev, I. F. Potapenko, and V. A. Chuyanov. Kinetic equations of the Landau type as a model of the Boltzmann equation and completely conservative difference schemes. *U.S.S.R. Comput. Maths. Math. Phys.*, 20, No.4, (1981) pp. 190–201.

[4] A. V. Bobylev. Exact solutions of the Boltzmann equation. *Dokl. Akad. Nauk. S.S.S.R.*, 225, (1975) pp. 1296–1299 (Russian).

[5] C. Buet, S. Cordier, P. Degond, and M. Lemou. Fast algorithms for numerical conservative and entropy approximations of the Fokker-Planck equation. *J. Comp. Phys.*, 133, (1997) pp. 310–322.

[6] C. Buet, S. Cordier. Numerical analysis of conservative and entropy schemes for the Fokker-Planck-Landau equation. To appear on *SIAM J. Num. Anal.*

[7] C. Buet, S. Cordier. Conservative and entropy decaying numerical schemes for the isotropic Fokker-Planck-Landau equation. *J. Comp. Phys.*, 145, No.1 (1998) pp. 228–245.

[8] P. Degond, B. Lucquin-Desreux. An entropy scheme for the Fokker-Planck collision of plasma kinetic theory. *Num. Math.*, 68, (1994) pp. 239–262.

[9] L. Desvillettes. On asymptotics of the Boltzmann equation when collisions become grazing. *Trans. Th. and Stat. Phys.*, 21, No.3 (1992) pp. 259–276.

[10] F. Filbet, L. Pareschi. Work in preparation.

[11] V. I. Lebedev. Explicit difference schemes with time variable steps for the solution of stiff system of equations. Sov. J. Numer. Anal. Math. Model. 4, No.2, 111-135 (1989)

[12] M. Lemou. Multipole expansions for the Fokker-Planck-Landau operator. *Num. Math.*, 68, (1998) pp. 597–618.

[13] M. Lemou. *C.R.A.S.*, 68, (1998) pp. 597–618.

[14] L. Pareschi, G. Russo, and G. Toscani. Méthode spéctrale pour l'équation de Fokker-Planck-Landau. *C.R.A.S. de Paris*.

[15] L. Pareschi, G. Russo. Numerical solution of the Boltzmann equation I: Spectrally accurate approximation of the collision operator. *SIAM J. Num, Anal.*

[16] L. Pareschi, G. Russo, and G. Toscani. Fast spectral methods for the Fokker-Planck-Landau collision operator of Plasma Physics. Submitted.

[17] M. S. Pekker, V. N. Khudik. Conservative difference schemes for the Fokker-Planck equation. *U.S.S.R. Comput. Maths. Math. Phys.*, 24, No.3, (1984) pp. 206–210.

[18] M. N. Rosenbluth, W. Macdonald, D.L. Judd, Fokker-Planck equation for an inverse-square force. *Phys. Rev. II*, 107, (1957) pp. 1–6.

[19] G. Sansone, Orthogonal functions, Coll. Pure and Applied Math., Vol 9, Intersc. Publisher (1959).

[20] C. Villani. On the Cauchy problem for Landau equations: Sequential stability, global existence. *J. Adv. Differ. Equ.*, 1, No.5, (1996) pp. 793–816.